New BIOTECHNOLOGY 79 (2024) 20–29

Contents lists available at ScienceDirect

New BIOTECHNOLOGY

journal homepage: www.elsevier.com/locate/nbt

# Inter-patient heterogeneity in the hepatic ischemia-reperfusion injury transcriptome: Implications for research and diagnostics

Silvia Groiss [a,1], Christian Viertler [a], Marcel Kap [b], Gerwin Bernhardt [c,d], Hans-Jörg Mischinger [c], Anieta Sieuwerts [e], Cees Verhoef [f], Peter Riegman [b], Mogens Kruhøffer [g], David Svec [h], Sjoback Robert Sjöback [i], Karl-Friedrich Becker [j], Kurt Zatloukal [a,*]

[a] Diagnostic & Research Institute of Pathology, Medical University of Graz, 8010 Graz, Austria
[b] Pathology Department, Erasmus University Medical Center, 3015CN Rotterdam, the Netherlands
[c] Division of General Surgery, Department of Surgery, Medical University of Graz, 8010 Graz, Austria
[d] Department of Orthopedics and Trauma Surgery, Medical University of Graz, 8010 Graz, Austria
[e] Department of Medical Oncology, Erasmus MC Cancer Institute and Cancer Genomics Netherlands, Erasmus University Medical Center, 3015CN Rotterdam, the Netherlands
[f] Department of Surgical Oncology, Erasmus MC Cancer Institute, Erasmus University Medical Center, 3015CN Rotterdam, the Netherlands
[g] BioXpedia A/S, 8200 Aarhus, Denmark
[h] Laboratory of Gene Expression, Institute of Biotechnology CAS, 252 50 Vestec, Czech Republic
[i] TATAA Biocenter AB, 411 03 Göteborg, Sweden
[j] Technische Universität München, 81675 München, Germany

ARTICLE INFO

*Keywords:*
Gene expression
Pre-analytical workflows
Microarray
Transplantation medicine
Biomarker

ABSTRACT

Cellular responses induced by surgical procedure or ischemia-reperfusion injury (IRI) may severely alter transcriptome profiles and complicate molecular diagnostics. To investigate this effect, we characterized such pre-analytical effects in 143 non-malignant liver samples obtained from 30 patients at different time points of ischemia during surgery from two individual cohorts treated either with the Pringle manoeuvre or total vascular exclusion. Transcriptomics profiles were analyzed by Affymetrix microarrays and expression of selected mRNAs was validated by RT-PCR. We found 179 mutually deregulated genes which point to elevated cytokine signaling with NFκB as a dominant pathway in ischemia responses. In contrast to ischemia, reperfusion induced pro-apoptotic and pro-inflammatory cascades involving TNF, NFκB and MAPK pathways. *FOS* and *JUN* were down-regulated in steatosis compared to their up-regulation in normal livers. Surprisingly, molecular signatures of underlying primary and secondary cancers were present in non-tumor tissue. The reported inter-patient variability might reflect differences in individual stress responses and impact of underlying disease conditions. Furthermore, we provide a set of 230 pre-analytically highly robust genes identified from histologically normal livers (<2% covariation across both cohorts) that might serve as reference genes and could be particularly suited for future diagnostic applications.

## 1. Introduction

Biospecimens, such as surgical specimens or biopsies are the key source of molecular information for basic and translational research as well as for molecular diagnostics and improving surgical procedures. Accumulating evidence suggests that pre-analytical variables of

*Abbreviations:* IRI, ischemia reperfusion injury; MC, MUG cohort; EC, EMC cohort; IPC, ischemic preconditioning; TVE, total vascular exclusion; CCC, cholangiocellular carcinoma; CRC, colorectal carcinoma; CV, covariation; CI, cold ischemia; WI, warm ischemia; DEG, differentially expressed genes; ECD, extended criteria donor; HCC, hepatocellular carcinoma; PPI, Protein-protein interaction; FFPE, formalin-fixed and paraffin-embedded; HE, hematoxylin-eosin; SPIDIA, Standardization and Improvement of Generic Pre-analytical Tools and Procedures for In Vitro Diagnostics; RMA, robust multi-chip average; NAT, normal-adjacent to tumor.

* Corresponding author.
*E-mail address:* kurt.zatloukal@medunigraz.at (K. Zatloukal).
[1] Department of Medicine IV, University Freiburg Medical Center, Faculty of Medicine, Freiburg University, 79106 Freiburg, Germany.

https://doi.org/10.1016/j.nbt.2023.12.001
Received 14 September 2023; Accepted 7 December 2023
Available online 10 December 2023

biospecimen, like effects of surgical procedures, ischemia and further processing, account for problems in reproducing scientific data and are responsible for the majority of laboratory diagnostic inaccuracies [1–3]. We have previously reported on protein and phosphoprotein as well as metabolome alterations to ischemia effects in liver tissue specimens that demonstrated some key proteins and metabolites, but also major inter patient variability [4]. However, whether the observed variability caused either by the patient or pre-analytical factors also influences transcriptional responses including the stability of RNA targets and may therefore affect molecular diagnostics, remains elusive. While unavoidable pre-analytical variables, such as fluctuations in gene expression due to individual genetic makeup (genotype), gender, age or disease, already compromise the reliability of laboratory results, extrinsic factors such as diverse surgical procedures add another layer of complexity. In hepatic tumor surgery, vascular occlusion is routinely performed to minimize operative haemorrhage, however at the expense of inducing ischemia and reperfusion injury (IRI) [5,6]. Response of organs to IRI is an almost unavoidable pre-analytical factor that adversely impacts molecular analyses of liver tissue and has severe implications for surgical procedures and preservation of organs during liver transplantation. The recent permission of extended criteria donor organs to minimize the number of patients awaiting liver transplantation clearly illustrates the need to better understand the pathogenesis of hepatic IRI in humans, in order to improve both patient management and rates of allograft acceptance [7–10]. The most common techniques for vascular occlusion are the Pringle manoeuvre (inflow occlusion) and total vascular exclusion (TVE, inflow and outflow occlusion) [11,12]. Furthermore, ischemic preconditioning (IPC) proved an effective strategy to attenuate IRI-associated liver damage and is clinically well-established [13,14]. How differences in these applied techniques affect transcriptional responses is still poorly investigated. Importantly, exuberant stress and inflammatory responses to IRI in liver specimen might mask transcriptional signatures of target transcripts ultimately hindering diagnosis of the underlying disease. Therefore, not only the transcriptional landscape of IRI needs to be investigated, but also a detailed understanding of analytical targets that are both unaffected by IRI and robust to additional pre-analytical variables is necessary.

To complement our previous studies on ischemia effects on the liver proteome and metabolome, the present study addresses the stability of transcriptional responses to several hepatic IRI conditions and in consideration of various pre-analytical variables at several time points during and after surgery [4,15]. By comparing two independent cohorts subjected either to the Pringle manoeuvre or TVE at two different medical centers in Graz (Austria) and Rotterdam (Netherlands), respectively, both mutually deregulated and stable genes, that might prove to be novel biomarkers suitable to assess IRI or disease severity in future studies, were investigated [16].

## 2. Materials and methods

### 2.1. Patients and study design

A total of 143 human liver samples representing different ischemia conditions were collected from 30 patients during and after routine liver surgery at the Medical University of Graz (MUG) and Erasmus Medical Centre Rotterdam (EMC) constituting the MUG cohort (MC) and EMC cohort (EC). The study was approved by the ethical committee of the MUG (reference number 20–066 and 14–173) and at EMC under reference number MEC-2008–397. Consent was obtained according to local procedures. The employed study design allows comparison of two different surgical techniques for liver resection due to primary and secondary tumors, thereby providing a real-life example of patient responses in two independent medical centers. Indication for liver surgery in patients was metastasis of colorectal cancer to the liver (CRC, n = 20), hepatocellular carcinoma (HCC, n = 3), cholangiocellular carcinoma (CCC, n = 3) or other diseases (other, n = 4, **Table 1**). The workflow is shown in Fig. 1A. All samples have been collected distant to the tumor and were immediately frozen in liquid nitrogen. In addition, biopsies were fixed in buffered 4% formaldehyde and embedded in paraffin for histopathological evaluation which was performed by experienced pathologists to assess absence of tumor or acute or chronic liver disease in H&E-stained slides. Liver steatosis was determined by using the Kleiner's scoring system for steatosis grades 1 (5%−33%), 2 (34–66%) and 3 (>66%). Based on the scoring obtained the MC was divided into to the "steatosis" sub-group (>20% steatosis) for simplified comparison to the "normal" sub-group (<5% steatosis) [17]. This step was made to create two clearly distinct sub-groups for analysis on the transcriptional level. Non-malignant tissue samples in the MUG cohort (MC) were collected before vessel clamping (t0, reference time point) using the Pringle manoeuvre as well as 30 min after vessel clamping (t1; warm ischemia), 30 min after reperfusion (t2; warm ischemia (WI) and reperfusion) and 30 min after tissue resection (t3; cold ischemia (CI), time between resection and fixation). In the EMC cohort (EC), samples were taken right with the first incision for tumor removal (t0′, reference time point), directly after excision (t0′ CI), after 30 min of CI (t30′) to validate findings in t3 of the MC, and at various time points thereafter (t60′, t120′, t180′ and t360′) to monitor the stability of RNA profiles during a potential procedural delay. No vessel clamping was applied in the EC because cutting was done with direct vessel sealing. CI samples were maintained in a humidified chamber during the testing period. Intraoperative WI times depend on the duration of the surgical procedure and vary between individual patients, potentially leading to increased variability in transcriptional profiles. In contrast, t1 samples (MC) were collected after a standardized WI time of 30 min. Specimen were cut to 5 × 5×5 mm and either snap frozen in cooled methyl butane (MC) or directly in liquid nitrogen (EC), in which it was subsequently stored until further analysis; or formalin-fixed and paraffin-embedded (FFPE), cut into 4 μm sections and stained using hematoxylin-eosin (HE) for morphological examination.

### 2.2. RNA extraction and quality control

Cryopreserved samples (n = 143) were shipped on dry ice to the SPIDIA consortium partner AROS for RNA extraction and microarray analysis. RNA was extracted using the miRNeasy Mini Kit (QIAGEN GmbH, Hilden, Germany) according to the manufacturer's instructions. Briefly, frozen liver samples (<50 mg) were transferred to 2 mL Safelock tubes on ice each containing 700 μL QIAzol and 2 steel balls, disrupted using a tissue lyser II and mixed with 140 μL chloroform. After phase separation by centrifugation, the upper aqueous phase was mixed with 1.5 volumes of 100% ethanol and passed over RNeasy Mini spin columns before centrifugation, washing steps in buffer RWT and RPE and elution in RNase free water. The concentration of each sample was calculated from the absorption at 260 nm and tested for purity using the 260 nm / 280 nm ratio on a Nanodrop XD-100. RNA integrity was verified using a 2100 Bioanalyzer (Agilent, Santa Clara, CA, USA).

### 2.3. Transcriptomics analysis and processing of raw data

300 ng RNA were used for transcriptomics using the GeneChip 3′ IVT Express Kit on Affymetrix Human Genome U219 array plates (all Affymetrix, Santa Clara, CA, USA) according to the manufacturer's instructions. A hybridization cocktail was mixed to the resulting final fragmented cRNA, hybridized to the array plates, washed and scanned on the GeneTitan System (ThermoFisher Scientific, Waltham, MA, USA). Quality control of microarray data was performed using Affymetrix Expression Console 1.3. RMA normalization (robust multi-chip average), background correction and quantile normalization across all arrays as well as median polished summarization based on log transformed expression values was conducted using the Partek Genomic suite v6.4 (Partek Inc., Chesterfield, MO, USA). A total of 49,387 probes were

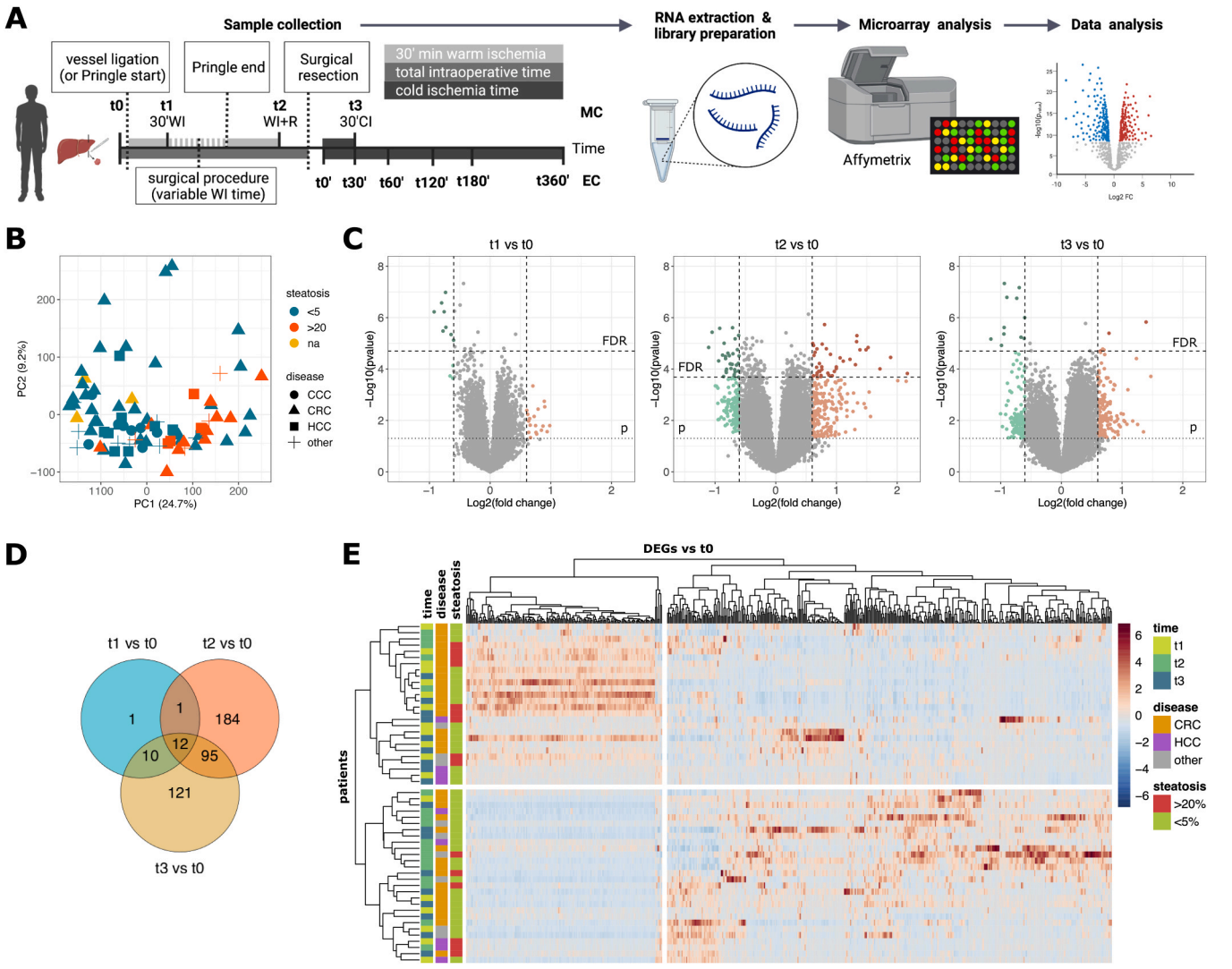


**Fig. 1.** Transcriptional response to IRI during and after surgery in MC. (A) Sampling scheme and workflows for MC and EMC cohort (EC). (B) PCA of MC samples. (C) Volcano plots of DEGs at t1, t2 and t3 compared to t0. (D) Venn diagram of DEGs. (E) Heatmap of DEGs normalized within each patient. Significance was considered at $p < 0.05$ (Welch t-test). Genes were considered de-regulated if FC was $> 1.5$ or $< -1.5$ with their p-values $< 0.05$. MC, MUG Cohort; EC, EMC Cohort; WI, warm ischemia; CI, cold ischemia; PC, principal component; CCC, cholangiocellular carcinoma; CRC, colorectal cancer; HCC, hepatocellular carcinoma; DEGs, differentially expressed genes.

evaluated and cleared for non-designated IDs resulting in overall 19,988 unique genes for further analysis.

### 2.4. Protein-protein interaction (PPI) network and functional annotation analysis

Functional analysis of differentially expressed genes (DEGs, fold change (FC) $> 1.5$ or $< -1.5$ and p-value $< 0.05$) was conducted using PANTHER's gene ontology enrichment analysis platform (www.geneontology.org) and run against the Homo sapiens reference list using Fisher's exact test [18,19]. The Kyoto Encyclopedia of Genes and Genomes (KEGG, https://www.genome.jp/kegg/) database was explored to identify highly affected pathways. Top significant GO terms and KEGG pathways, selected if FDR $< 0.05$, were visualized in R using the ggplot2 () package. Protein-protein interaction (PPI) networks of DEGs illustrated using the STRING online database (Version 11.5; https://string-db.org/) [20]. Additionally, the integrative annotation analysis tool Metascape (https://metascape.org/gp/index.html#/main/step1) was used for functional analysis of biological processes (GO) and pathways (KEGG) of DEGs mutually deregulated in both cohorts using a minimum enrichment score of 1.5, an adjusted p-value of $< 0.05$ and a minimum overlap of three genes. Representative terms are presented by circle nodes, whose size is proportional to the number of genes under that term. Same colors of multiple terms belong to the same cluster. Terms with a similarity score of $> 0.3$ are linked by an edge, where the thickness of the edge represents the similarity score itself.

### 2.5. Selection of candidate genes and assay design

The top DEGs were identified at each center and validated on both cohorts by quantitative real-time polymerase chain reaction (RT-PCR). In total, five up- and five downregulated genes (from data of CRC metastasis group with $< 5\%$ steatosis) and five stable, potential reference genes (from whole data set including all patients and time points) were selected at each medical center (three downregulated at EC). Ubiquitous gene and protein expression in different tissue types was additionally checked in databases (www.genecards.org, www.proteinatlas.org). RT-PCR assays for these selected genes were designed to have good linearity (5 log dynamic range and low error measured as the mean square error of the data points fit to the regression line), high

efficiency (>80%), specific amplification of cDNA (no amplification of gDNA or at least five cycles difference between target and genomic Cq-value) and negative NTCs (No Template Controls) in 40 cycles of PCR. Primers were, where applicable, designed into neighbor exons separated by at least a 500 bp intron to increase specificity and cover a length of 80–150 base pairs (bp). All assays were initially tested for specificity using SYBR green (Thermo Fisher Scientific). All primer design was performed with Primer BLAST followed by probe design with Beacon Designer (PREMIER Biosoft International, Palo Alto, Canada, Suppl. Table S11).

### 2.6. Data analysis and statistics

Statistical analysis and data representation was performed in Partek Genomic suite v6.4, GraphPad Prism (version 9.3.1) and R (version 4.1.2). Statistical differences between two groups were assessed by two-tailed Student's t-test between the individual time points (t1–3; t30′-t360′) and the reference time point of each cohort (t0). R packages prcomp, ggvenn and pheatmap were used for principal component analysis (PCA), Venn diagram and heatmap preparation, respectively. Significant deregulation was considered at a fold change (FC) of $> 1.5$ or $< -1.5$ and $p < 0.05$ or false discovery rate (FDR) $< 0.05$ where appropriate, as indicated in each graph. FDR was calculated using the Benjamini-Hochberg method. RT-PCR was performed in technical triplicates (MC) or duplicates (EC), and normalized to GAPDH and the reference time point t0/t0′ of each individual patient.

## 3. Results

### 3.1. Transcriptomic hallmarks of IRI during and directly after surgery in MC

Principal component analysis (PCA) of the entire MUG cohort (MC) data set showed substantial heterogeneity in non-tumor liver samples between patients, even already at t0, which illustrates the strong influence of the patient's genetic background, underlying disease and particularly the grade of steatosis, as evidenced by the shift in PC1 (Fig. 1B, Suppl. Fig. S1). Expression analysis revealed a total of 423 differentially expressed genes (DEGs) across all tested time points (from a total of 19,988 unique genes) that occurred primarily after reperfusion (t2) and largely persisted until cold ischemia (t3; Fig. 1C-D). DEGs of all time points are summarized in Suppl.Table S1; input genes for Fig. 1D are given in Suppl. Table S2. The top 30 genes with the greatest fold-change per time point are summarized in Suppl. Table S3. Next, to identify commonalities in responses to IRI impartial of the observed heterogeneity at basal expression, we normalized the data of each patient to the respective reference time point (t0) and evaluated the association between the underlying disease, grade of steatosis and time points using unsupervised clustering. We identified two subclasses of genes primarily separating time points t1 and t3 (upper class) from t2 (lower class) suggesting a deviating nature of genes induced by ischemia compared to reperfusion (Fig. 1E). Interestingly, signatures in t1 and t3 within one patient were more similar than effects induced by IRI leading to their clustering in most patients. Consequently, since neither disease or grade of steatosis nor effects of circulatory or oxygen deprivations induced by the Pringle manoeuvre caused distinct clustering, we conclude that the patient's basal transcriptional signature constitutes the prevalent factor.

### 3.2. Importance of TNF, MAPK and NFκB signaling in hepatic IRI

DEGs identified in t2 and t3 in the MC were further functionally analyzed to identify biological processes and related pathways involved in hepatic IRI by using GO and KEGG enrichment analysis. Biological processes related to programmed cell death and apoptosis clearly dominated in both t2 and t3 (both three out of top five GO terms), confirming previous reports on the molecular pathogenesis of IRI (Fig. 2A-B).[8,21] Reperfusion additionally enriched several GO terms related to protein folding that are characteristic for members of the DnaJ and HSP heat shock protein families, further pointing towards elevated oxidative stress. KEGG enrichment analysis revealed TNF and MAPK signaling as the dominant contributing pathways at t2 and corroborated the importance of NFκB signaling in IRI-induced inflammation. These findings on transcriptome level are in line with reports in rodents and were recently confirmed by analysis of three available microarray data sets of human pre-ischemic and re-perfused liver biopsies [22–24]. Furthermore, this data supports our previous study on the protein and phosphoprotein levels conducted on samples of a sub-cohort of the current study demonstrating that with increased duration of ischemia there was an increase in protein expression of MAPK and NFκB as well as an increase in phosphorylated NFκB (Fig. 2C).[4,25].

Notably, the TNF and MAPK but not NFκB signaling pathways disappeared in the top 20 KEGG pathways in t3 (Fig. 2D), while terms for immune regulation and inflammation were enriched. GO terms and KEGG pathways identified in our analysis are summarized in Tables S4 and S5.

### 3.3. Tumor-free tissues reveal cancer signatures against the background of IRI

Interestingly, both t2 and t3 revealed enrichment in pathways associated with cancer ('Pathways in cancer', 'Transcriptional misregulation in cancer') despite a lack of morphological evidence of tumor tissue in the samples analyzed (Fig. 2C-D). Moreover, our data revealed enrichment of genes involved in CRC ('Colorectal cancer'), the underlying disease of the majority of patients in the MC (Fig. 2C, Table 1), even in the presence of a strong response to IRI (Suppl. Table S5).

### 3.4. Steatosis in IRI may affect AP-1 activation

We next explored the basal transcriptional dysregulation between steatotic and non-steatotic (normal) livers that we had already observed in the PCA (Fig. 1B, Fig. 3A). We normalized data to t0 within each patient and calculated fold deregulation at t2 and t3, based on which we assessed Δfold change scores between the two sub-groups (Fig. 3B, Suppl.Table S6). Expression of several genes doubled in both t2 and t3, including FBLN1, MGP and members of the ADAMTS protease family that are highly associated with extracellular matrix remodeling and degradation [26–29]. However, and contrary to previous reports in rodents, we observed affected genes to be almost entirely down-regulated in steatotic compared to normal livers at both t2 and t3. These included for example FOS, JUN and DUSP1 suggesting reduced activation of the AP-1 transcription factor in the pathophysiological changes observed in steatotic IRI (Fig. 3C-D, Suppl. Table S7) [30–32]. The interconnectivity of down-regulated genes is illustrated using the STRING database (Fig. 3E). Associated GO terms involved processes related to signaling by external stimuli and regulation of cell death (Fig. 3F). Interestingly, the most significant GO term ('cellular response to chemical stimulus') included genes such as DUSP1 (glucose metabolism), GDF15 (non-alcoholic steatohepatitis), DDIT4 (MAPK signaling and steatosis) and FGF21 (lipid metabolism) that highly relate to liver steatosis. Major KEGG pathways involved Toll-like receptor signaling, MAPK signaling and cytokine-cytokine receptor interaction (Fig. 3G).

### 3.5. Common deregulated genes in IRI in two different cohorts foster cell death-initiating programs

To identify molecular responses to hepatic IRI independent of the surgical technique and local workflows, we validated the DEGs identified in the MC using the EMC cohort (EC) as an independent cohort, in which TVE was applied instead of the Pringle manoeuvre and IPC. Conformable with the MC, PCA of the EC revealed substantial inter-

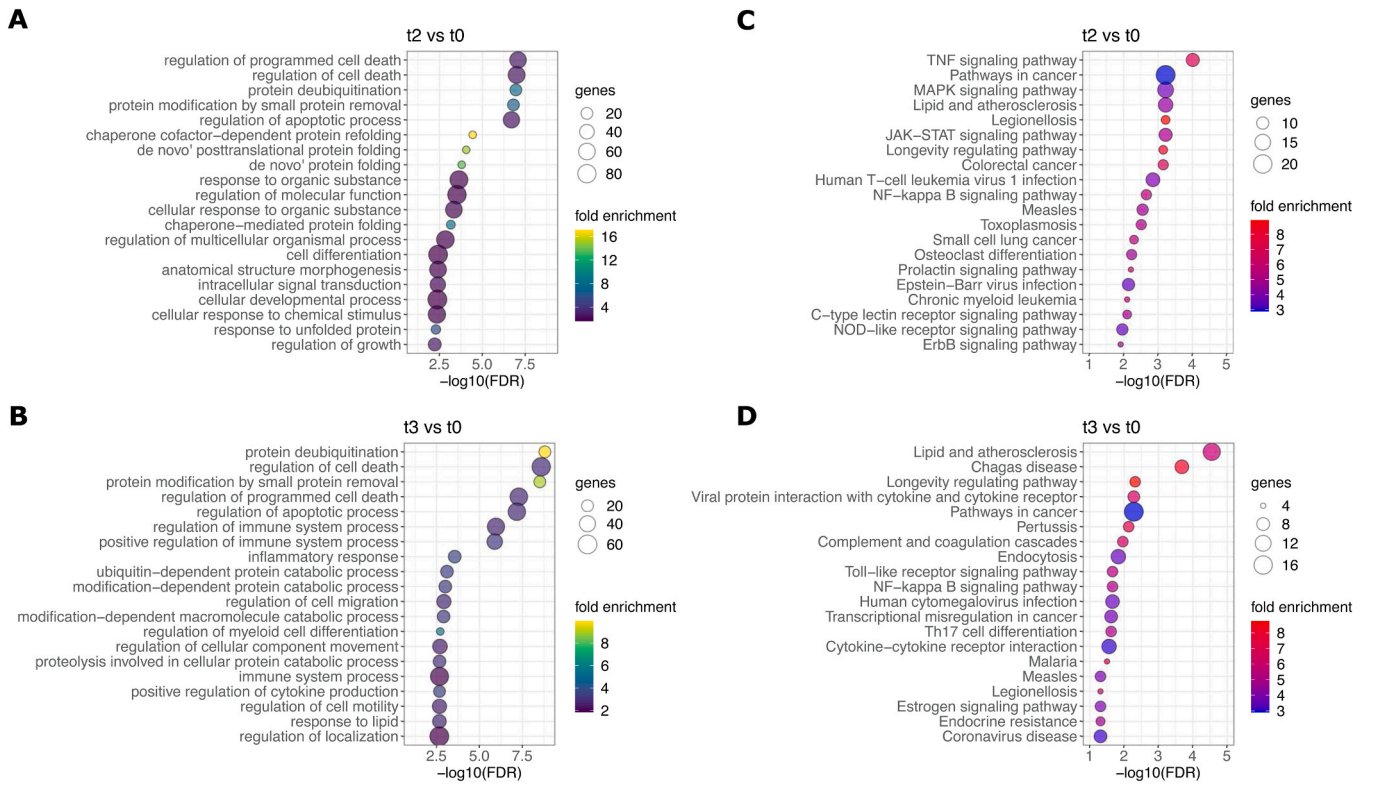


**Fig. 2.** Top 20 GO terms and KEGG pathways of DEGs in MC. (A, B) GO enrichment and (C, D) KEGG analysis performed on DEGs in (A, C) t2 and (B, D) t3 compared to t0.

patient heterogeneity in IRI responses at all tested time points (Fig. 4A). To justifiably compare these two cohorts, mRNA analysis was performed in the same laboratory using the same platform with identical criteria for DEG assessment (FC $> 1.5$ or $< -1.5$ and p-value $< 0.05$). We found a total of 1145 genes to be up- (673 genes) or down-regulated (472 genes) in the EC after 30 min of CI (t30′), as opposed to 277 DEGs at the same time point (t3) in the MC (Fig. 4B, Fig. 1C). Notably, the vast majority of DEGs remained dysregulated throughout the entire 6 h (t360′) CI period (Suppl. Table S8, Suppl. Fig. S2). Overall, 146 and 33 genes were mutually up- or down-regulated in both cohorts, respectively (Fig. 4C, Suppl. Table S9). The top 30 genes with the greatest fold changes in t0′WI and t30′ are summarized in Suppl. Table S10.

Commonly deregulated genes were further tested for biological functions and processes using the gene annotation and analysis platform Metascape (Fig. 4D). 'Cytokine signaling in immune system' was the dominant process (nodes represent enriched terms; edges represent similarity scores), fostering reperfusion-induced pro-inflammatory signaling as the main driver for hepatic IRI. Expanded analysis on enriched pathways confirmed NFκB, TNF, Toll-like and MAPK signaling as key regulating cell damage and death-initiating cascades (Fig. 4E), while most enriched biological processes related to stress and apoptosis ($n = 8$ out of top 20 terms; Fig. 4F). Other processes were vascular wound healing and permeability as well as endothelial cell differentiation, implying transcriptional responses directed at restoring the integrity of damaged vasculature.[33] Intriguingly, fold enrichment scores for 'Colorectal cancer' signatures and 'Pathways in cancer' almost doubled in conjoint analysis of the tumor free liver samples, probably due to the increased ratio of CRC patients upon inclusion of the EC in the analysis ($n = 9$; 100% CRC patients in EC, Table 1).

### *3.6. Inter-patient heterogeneity complicates molecular analyses in hepatology*

Finally, we tested whether robustly up- and down-regulated, as well as stable genes selected from each cohort ($n = 3$–5 each) might prove suitable as potential biomarkers for IRI. Up-regulated genes were generally more elevated in the EC than in the MC at t3/t30′, probably due to IPC in the MC (Fig. 5A). Down-regulated genes selected from the MC were conjointly reduced in both cohorts, which was not the case for genes selected by the EC (Fig. 5B). Even stable genes showed marked heterogeneity across both MC and EC (Suppl. Fig. S3). Covariation analysis (CV) revealed substantial differences in the expression magnitude between patients as well as between the two cohorts, complementing our initial findings on inter-patient heterogeneity (Fig. 5C). Nonetheless, selected candidate genes were validated by RT-PCR (Suppl. Table S11). We observed marked differences in target expression levels across the patients primarily during ischemia and reperfusion (MC) that seemed to level out during CI (EC). Fig. 5D illustrates the extent of inter-patient variability of four representative target genes over the entire study period.

Importantly, we additionally identified 230 stable genes with less than 2% CV across both cohorts that were not deregulated by IRI or CI, and might therefore be explored as potential reference genes or biomarker candidates that are essentially robust to pre-analytical variables, and therefore useful for possible clinical application (Suppl. Table S12). Raw data of selected stable genes is given in Suppl. Table S13.

## 4. Discussion

This study aimed at investigating alterations of transcriptional profiles of human livers during warm ischemia, IRI and CI in two independent cohorts (MC, Graz and EC, Rotterdam) subject to different surgical procedures (IPC and Pringle manoeuvre in MC, TVE in EC), which complements our previous studies on the protein / phosphoprotein and metabolome profiles of a sub-cohort of the present study on liver specimens that have been processed following the same study protocol [4,15]. To justifiably assess transcriptional alterations caused

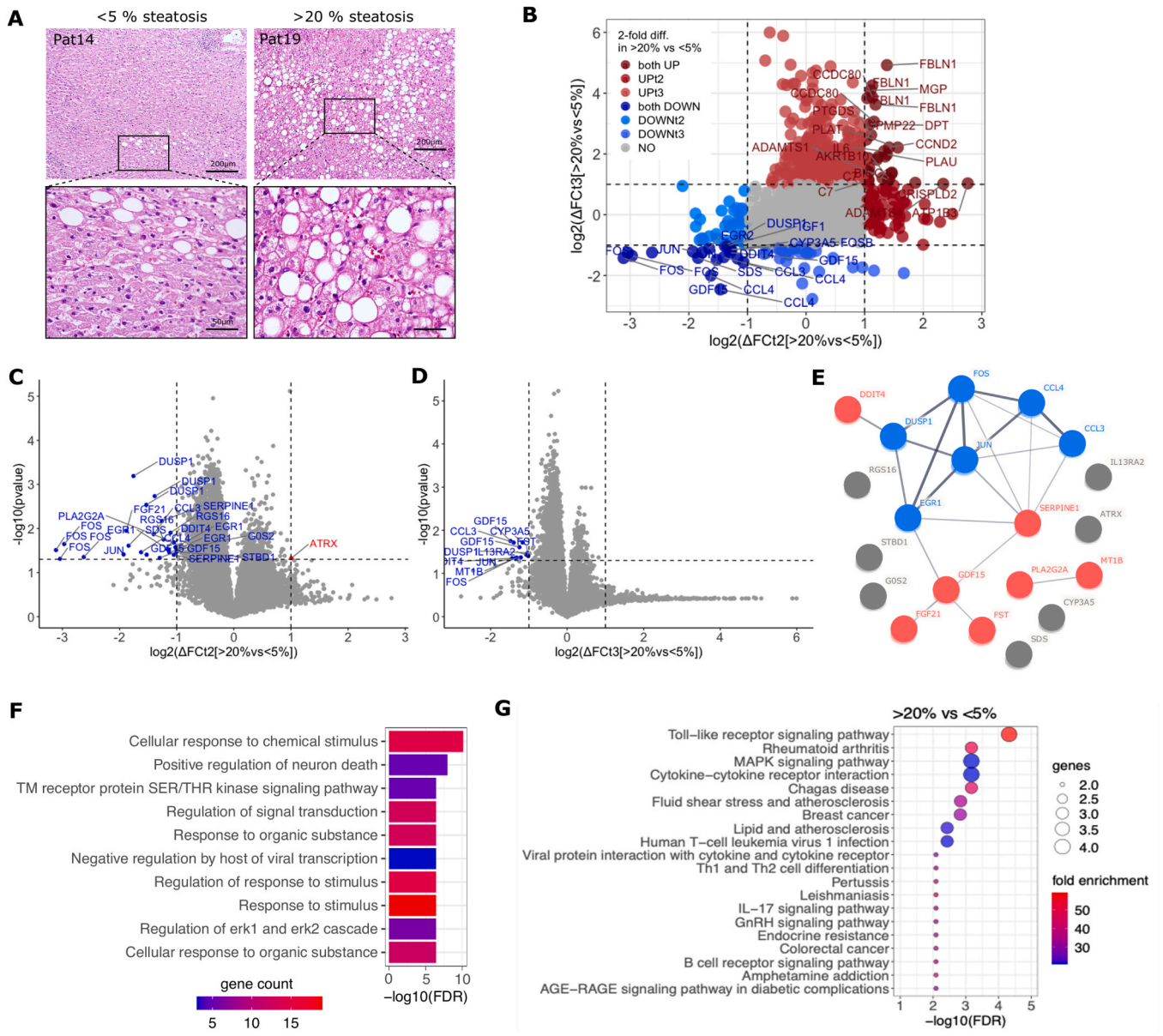


**Fig. 3.** Differential gene regulation in IRI and steatotic livers in MC. (A) Representative HE images of steatotic (>20%) and normal (<5%) sub-groups. (B) Fold regulation and (C, D) DEG analysis of t2 and t3 between the sub-groups. (E) Protein-protein interaction (PPI) network of down-regulated genes, nodes represent proteins, connecting lines represent confidence level of data support (cut-off criterion > 0.4 (red) and > 0.9 (blue)). (F) GO biological processes involving DEGs in steatosis. Significance considered at $p < 0.05$ (Welch t-test). (G) KEGG analysis of DEGs in steatosis.

by pre-analytical effects such as surgical procedures, ischemia periods, or disease condition, RNA analysis was performed in the same laboratory using identical protocols. Initial analysis generally indicated lower transcriptional deregulation in the MC compared to the EC, most likely mitigated by IPC that was not applied in the latter. Expression analysis of the MC revealed that a majority of genes remained unaffected by both ischemia or reperfusion, narrowing down the otherwise extensive complexity of IRI to a few but highly influential pathways. In fact, ischemia alone did not elicit major changes in gene expression in our study, supporting previous findings [34]. Reperfusion on the other hand, triggered TNF and MAPK signaling pathways that are considered responsible for pro-inflammatory and pro-apoptotic or -necroptotic processes in hepatic IRI [8,21,25]. Activation of these pathways based on analysis of mRNA expression levels in MC data followed an expected time-course because inflammation-related GO terms were only detectable in CI samples collected at least 1–3 h after reperfusion (t3). Interestingly, the disappearance of the TNF and MAPK signaling pathways at t3 (CI) along with the emergence of the Toll-like receptor signaling pathway and up-regulation of *GADD45* family members (*GADD45B*, *GADD45G*) supports previous findings that propose the suppression of TNF-dependent pro-inflammatory processes by NFκB signaling [35]. NFκB activation balances apoptosis and necroptosis in cancer and plays a crucial role in necroptosis in hepatic IRI [36–38]. TNF and NFκB pathway enrichment in hepatic IRI was recently also shown using three independent microarray data sets of human pre-ischemic and reperfused biopsies from liver transplant patients by evaluating the intersecting DEGs [22]. Additionally, this is in line with our previous protein analysis demonstrating increased MAPK and NFκB protein expression and phosphorylation levels [4]. Hence, NFκB may constitute an important target for further studies in particular as it mitigates exacerbated necroptosis in steatotic livers in IRI, which comprise an ever-increasing proportion of donor grafts [34,35]. However, although induction of MAPK and NFκB signaling in hepatic IRI has also been observed on protein level in our previous study supporting the transcriptome data at

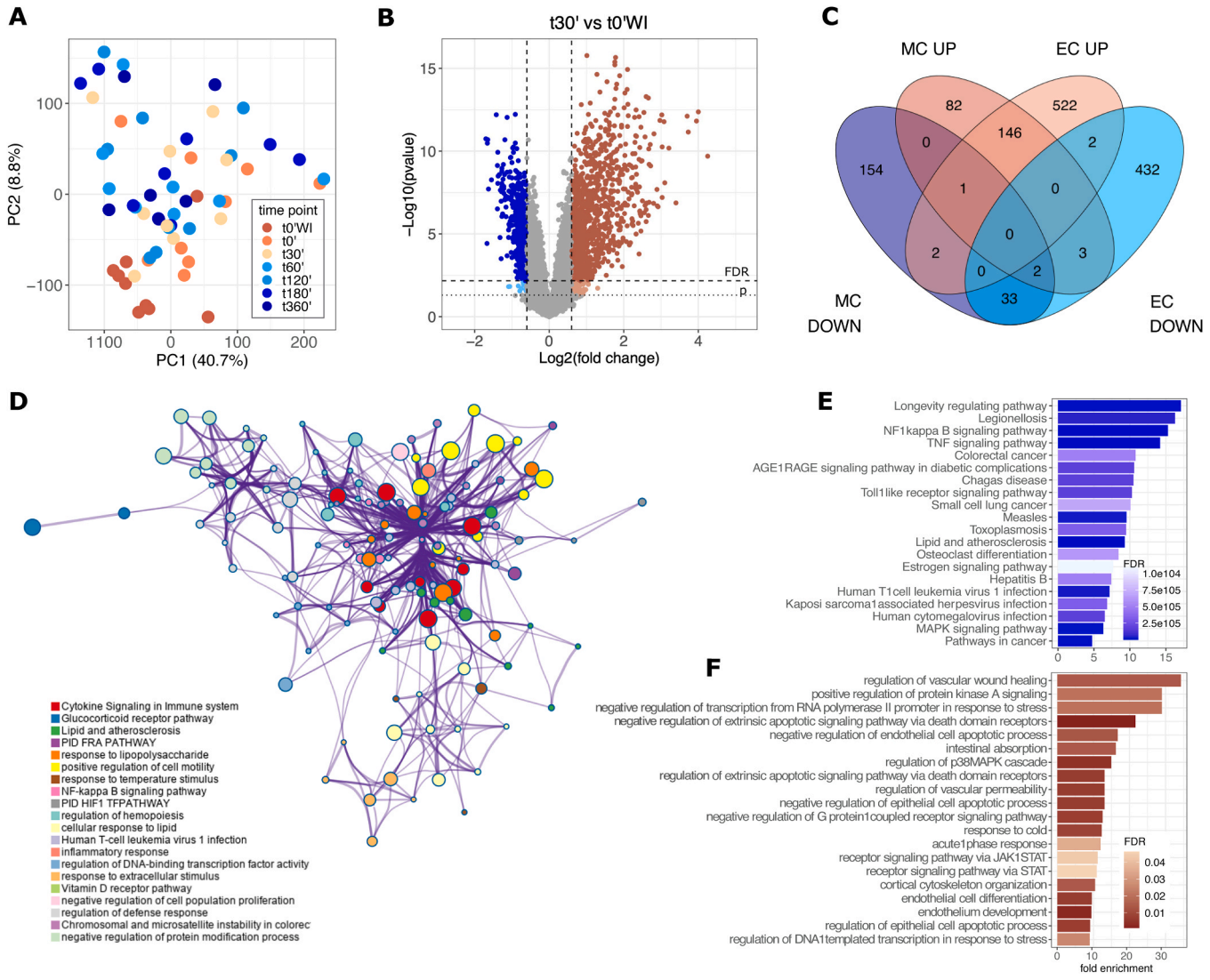


**Fig. 4.** Comparative analysis of MC and EC deregulated genes. (A) PCA of EC. (B) Volcano plot of t30' vs t0'WI. (C) Venn diagram of 146 and 33 mutual DEGs in MC and EC. Down-regulated genes are colored in blue, up-regulated genes are colored in red. (D) Metascape analysis and (E) KEGG as well as (F) GO enrichment analysis of 179 mutually DEGs. Statistical significance was assessed by Student's t-test with unequal variances (Welch t-test, * $p < 0.05$). MC, MUG cohort; EC, EMC cohort; NFκB, nuclear factor 'kappa-light-chain-enhancer' of activated B-cells; TNF, tumor necrosis factor; MAPK, mitogen-activated protein kinase.

hand, both our studies highlight the pronounced interpatient variability in signal intensities both on the range and time of their induction clearly demonstrating the complex situation posed to diagnostics using biospecimen, which this study aims to emphasize. Their widespread use calls for further in-depth analysis to help standardize molecular diagnostics and support endeavors directed at personalized medicine [4].

We further analyzed steatotic livers as these comprise an increasing proportion of donor grafts [39]. Our data derived from such liver specimen indicates genes to be markedly down-regulated (for example *FOS, JUN, DUSP1*) compared to normal samples at both t2 and t3 (Fig. C-D). Indeed, downregulation of FOS, JUN and DUSP1 may condition failure of steatotic allografts, as their transcriptional regulation affects activation of the cell-death regulating transcription factor activator protein 1 (AP-1). Furthermore, co-expression of *FOS/JUN* is required for adequate tissue repair following hepatic IRI, while *DUSP1 (MKP-1)* maintains glucose and energy homeostasis [30,40–43]. Collectively, the reduced activity of AP-1 along with distorted energy levels might prime steatotic livers for necroptosis without the means for sufficient tissue repair following transplantation, overall initiating degenerative processes in steatosis that normal livers might be able to compensate.

Interestingly, several DEGs identified in our study (*FOS, JUN, EGR1, DUSP1*) were also deregulated in renal IRI [44]. These hub genes might therefore represent general responses to IRI in multiple organs and advocate for further studies on the role of AP-1 and its association to necroptosis in steatotic conditions [45]. Notably, pathway analysis in the MC also revealed cancer signatures to be highly enriched despite the use of tumor-free tissue in our analysis. These findings together with our previous work on cancer-related signatures in livers with steatohepatitis, as well as comprehensive analysis of the unique 'normal adjacent to tumor' (NAT) transcriptome, highlight on the one hand some caveats for use of NAT biospecimen for basic research (e.g., data referring to so called "normal" liver), and on the other hand open new diagnostic purposes concerning systemic disease effects [46,47].

Moreover, validation of the results from the MC using the EC to identify responses independent of the applied surgical technique revealed a substantial number of genes to be similarly deregulated, indicating the common denominators of the general stress and pro-inflammatory response to IRI. These reiterated the fundamental role of NFκB and TNF signaling in hepatic IRI including cytokine signaling in the immune system and multiple stress- and apoptosis-related processes. Although the vast majority of DEGs elicited profound stability

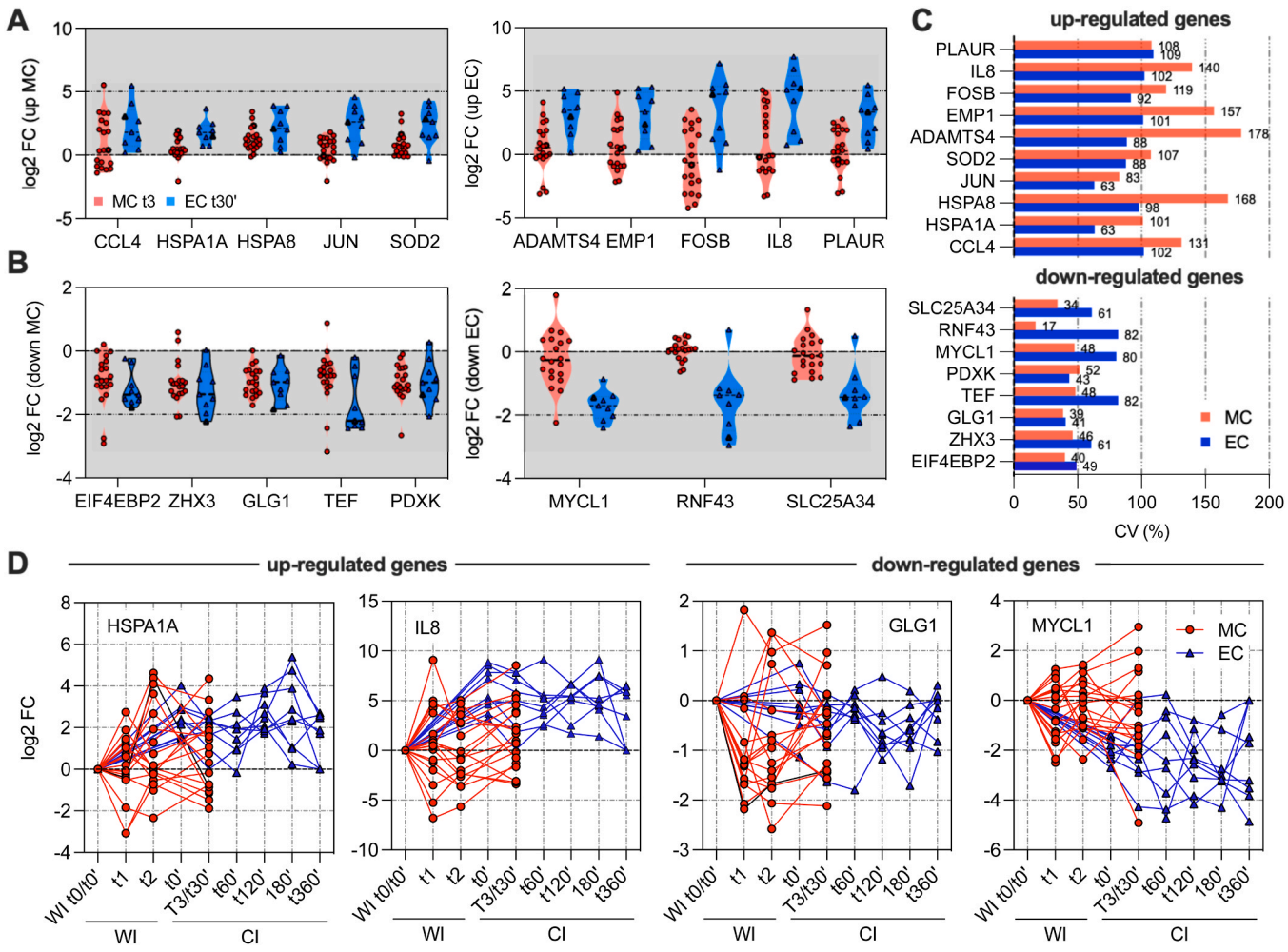


**Fig. 5.** Individual variability of selected deregulated genes validated by RT-PCR. (A, B) Examples of (A) up- and (B) down-regulated genes at t3/t30′ per cohort identified in bulk analysis. (C) Covariation of gene microarray data at t3/t30′ calculated across all patients per cohort. (D) RT-PCR of representative up-regulated (HSPA1A in MC and IL8 in EC) and down-regulated (GLG1 in MC and MYCL1 in EC) genes across all time points.

throughout the entire 6 h of CI (t360′), rendering the targets suitable for analytical purposes in transplantation medicine, the marked inter-patient heterogeneity also highlighted the limitations for identifying generic biomarkers for hepatic IRI (Suppl. Fig. S3B) [48]. Precisely, the substantial transcriptional heterogeneity observed in both cohorts already at t0 strongly suggests the patient's genetic background and disease condition to be the main factors determining individual transcriptome profiles, rather than pre-analytical effects caused by intra-operative time or surgical technique (Fig. 1E). In this context it is interesting to note that the previous NMR-based metabolomics study performed on a sub-cohort demonstrated a similar time-course of the overall metabolomics signatures indicating similar exposure to ischemia injury of the study group. Therefore, the inter-patient variability observed in this study on the transcriptome level, and the previous study on the phosphoproteome suggest that these variabilities are not a result of different exposures but rather reflect different individual responses to a similar injury [4,15]. Collectively, up-regulated genes showed more CV than down-regulated genes, indicating that IRI- and CI-induced gene expression dominates over gene repression or RNA degradation. Additionally, we identified 230 genes unaffected by hepatic IRI or CI that were robust to key pre-analytical effects. Due to the strong interpatient variability in IRI observed in our cohorts, it is of particular interest to further analyze these stable genes and identify potential reference genes or novel molecular markers for certain disease conditions that still lack biomarkers in clinical settings.

## 5. Conclusion

Overall, on one hand this study provides a comprehensive transcriptome data set of the human in vivo liver transcriptome with minimal pre-analytical effects (i.e., t0 samples). On the other hand, results obtained during the course of surgery denominate fundamental molecular mechanisms of hepatic IRI in humans. While these findings are still preliminary and require further validation, understanding the demonstrated interpatient variability and major systemic effects of for example local lesions, such as primary and secondary liver tumors in histopathological normal tissue is paramount and calls for additional validation on both transcriptome and proteome levels. Finally, the strong inter-patient variability in particular emphasizes the role of the individual patient`s medical and genetic history, which this study advocates to be more considered in molecular analyses and requires proper documentation underlining requirements of ISO standards for the pre-examination process (pre-analytics) for molecular diagnostics, and the European in vitro diagnostic regulation [49].

## Funding

This study was supported by the European Commission funded project SPIDIA (Standardization and Improvement of Generic Pre-analytical Tools and Procedures for In Vitro Diagnostics; www.spidia.eu, grant agreement Nr. 222916).

## CRediT authorship contribution statement

KZ, ChV. Sample collection: ChV, MK, GB, HJM, CV. Data acquisition: MK, KW, CV, AS, MoK, RS, DS. Statistical analysis: KW, SG, AS, MoK. Funding acquisition: KZ. Data analysis and interpretation: KZ, SG, PR, CV, KFB. Writing – original draft: SG, CV, PR, KFB. Writing – review & editing: KZ, SG, PR, ChV. Study supervision: KZ. All authors reviewed and approved the manuscript.

## Declaration of Competing Interest

KZ is founder and CEO of Zatloukal Innovations GmbH. RS is employed by TATAA Biocenter AB. MK is employed by BioXpedia A/S, which has no commercial interest in the results of the present publication.

## Data availability

The entire data set is already uploaded on NCBI GEO and locked. It will be made publicly available upon acceptance of the paper. Reviewers can have access to the data beforehand.

## Acknowledgments

We thank Karin Wagner for DNA-Array data analysis, Monika Moser and Daniela Pabst for performing RT-PCR analysis and Dr. Penelope Kungl for critically reading the manuscript.

*Informed consent statement*

Informed consent was obtained from all subjects involved in the study.

## Supporting informations

Supplementary data associated with this article can be found in the online version at XXX. Fig. S1: PCA of t0 of MC; Fig. S2: KEGG analysis of DEGs in steatosis; Fig. S3: Response to IRI in EC at various time points; Fig. S4: Stable genes. Table S1: DEGs MC; Table S2: Genes Venn diagram; Table S3: TOP30 genes MC; Table S4: GO MC; Table S5: KEGG MC; Table S6: Steatosis FC; Table S7: Steatosis DEGs; Table S8: DEGs EC; Table S9: Venn EC-MC; Table S10: TOP30 genes EC; Table S11: Primer RT-PCR; Table S12: Stable genes CV 2%; Table S13: Stable genes Rawdata.

## Appendix A. Supporting information

Supplementary data associated with this article can be found in the online version at doi:10.1016/j.nbt.2023.12.001.

## References

[1] Lippi G, Banfi G, Church S, Cornes M, de Carli G, Grankvist K, et al. Preanalytical quality improvement. In pursuit of harmony, on behalf of European Federation for Clinical Chemistry and Laboratory Medicine (EFLM) Working group for Preanalytical Phase (WG-PRE). Clin Chem Lab Med 2015;53. https://doi.org/10.1515/cclm-2014-1051.

[2] Hawkins R. Managing the pre- and post-analytical phases of the total testing process. Ann Lab Med 2012;32:5–16. https://doi.org/10.3343/alm.2012.32.1.5.

[3] Compton CC, Robb JA, Anderson MW, Berry AB, Birdsong GG, Bloom KJ, et al. Preanalytics and precision pathology: pathology practices to ensure molecular integrity of cancer patient biospecimens for precision medicine. Arch Pathol Lab Med 2019;143:1346–63. https://doi.org/10.5858/arpa.2019-0009-SA.

[4] Gündisch S, Hauck S, Sarioglu H, Schott C, Viertler C, Kap M, et al. Variability of protein and phosphoprotein levels in clinical tissue specimens during the preanalytical phase. J Proteome Res 2012;11:5748–62. https://doi.org/10.1021/pr300560y.

[5] Chouillard EK, Gumbs AA, Cherqui D. Vascular clamping in liver surgery: physiology, indications and techniques. Ann Surg Innov Res 2010;4:2. https://doi.org/10.1186/1750-1164-4-2.

[6] Nardo B, Ercolani G, Montalti R, Bertelli R, Gardini A, Beltempo P, et al. Hepatic resection for primary or secondary malignancies with involvement of the inferior vena cava: is this operation safe or hazardous? J Am Coll Surg 2005;201:671–9. https://doi.org/10.1016/j.jamcollsurg.2005.06.272.

[7] Mihaylov P, Mangus R, Ekser B, Cabrales A, Timsina L, Fridell J, et al. Expanding the donor pool with the use of extended criteria donation after circulatory death livers. lt.25462 Liver Transplant 2019. https://doi.org/10.1002/lt.25462.

[8] Peralta C, Jiménez-Castro MB, Gracia-Sancho J. Hepatic ischemia and reperfusion injury: effects on the liver sinusoidal milieu. J Hepatol 2013;59:1094–106. https://doi.org/10.1016/j.jhep.2013.06.017.

[9] Mendes-Braz M, Elias-Miró M, Jiménez-Castro MB, Casillas-Ramírez A, Ramalho FS, Peralta C. The current state of knowledge of hepatic ischemia-reperfusion injury based on its study in experimental models. J Biomed Biotechnol 2012;2012:1–20. https://doi.org/10.1155/2012/298657.

[10] Wenzel N, Blasczyk R, Figueiredo C. Animal models in allogenic solid organ transplantation. Transplantology 2021;2:412–24. https://doi.org/10.3390/transplantology2040039.

[11] Abdalla EK, Noun R, Belghiti J. Hepatic vascular occlusion: which technique? Surg Clin North Am 2004;84:563–85. https://doi.org/10.1016/S0039-6109(03)00231-7.

[12] PRINGLE JH. Notes on the arrest of hepatic hemorrhage due to trauma. Ann Surg 1908;48:541–9. https://doi.org/10.1097/00000658-190810000-00005.

[13] Clavien P-A, Yadav S, Sindram D, Bentley RC. Protective effects of ischemic preconditioning for liver resection performed under inflow occlusion in humans. Ann Surg 2000;232:155–62. https://doi.org/10.1097/00000658-200008000-00001.

[14] Sola A, Alfaro V, Hotter G. Intestinal ischemic preconditioning: less xanthine accumulation relates with less apoptosis. Apoptosis 2004;9:353–61. https://doi.org/10.1023/B:APPT.0000025812.45382.4d.

[15] Cacciatore S, Hu X, Viertler C, Kap M, Bernhardt GA, Mischinger H-J, et al. Effects of intra- and post-operative ischemia on the metabolic profile of clinical liver tissue specimens monitored by NMR. J Proteome Res 2013;12:5723–9. https://doi.org/10.1021/pr400702d.

[16] Riegman PHJ, Becker KF, Zatloukal K, Pazzagli M, Schröder U, Oelmuller U. How standardization of the pre-analytical phase of both research and diagnostic biomaterials can increase reproducibility of biomedical research and diagnostics. N Biotechnol 2019;53:35–40. https://doi.org/10.1016/j.nbt.2019.06.007.

[17] Kleiner DE, Brunt EM, van Natta M, Behling C, Contos MJ, Cummings OW, et al. Design and validation of a histological scoring system for nonalcoholic fatty liver disease. Hepatology 2005;41:1313–21. https://doi.org/10.1002/hep.20701.

[18] Carbon S, Douglass E, Good BM, Unni DR, Harris NL, Mungall CJ, et al. The gene ontology resource: enriching a gold mine. Nucleic Acids Res 2021;49:D325–34. https://doi.org/10.1093/nar/gkaa1113.

[19] Ashburner M, Ball CA, Blake JA, Botstein D, Butler H, Cherry JM, et al. Gene ontology: tool for the unification of biology. Nat Genet 2000;25:25–9. https://doi.org/10.1038/75556.

[20] Szklarczyk D, Gable AL, Lyon D, Junge A, Wyder S, Huerta-Cepas J, et al. STRING v11: protein–protein association networks with increased coverage, supporting functional discovery in genome-wide experimental datasets. Nucleic Acids Res 2019;47:D607–13. https://doi.org/10.1093/nar/gky1131.

[21] Weigand K, Brost S, Steinebrunner N, Büchler M, Schemmer P, Müller M. Ischemia/reperfusion injury in liver surgery and transplantation: pathophysiology. HPB Surg 2012;2012:1–8. https://doi.org/10.1155/2012/176723.

[22] Guo J, Han S, Chen Q, Wang T, Yu B, Zhou J, et al. Analysis of potential immune-related genes involved in the pathogenesis of ischemia-reperfusion injury following liver transplantation. Front Immunol 2023;14. https://doi.org/10.3389/fimmu.2023.1126497.

[23] Ocuin LM, Zeng S, Cavnar MJ, Sorenson EC, Bamboat ZM, Greer JB, et al. Nilotinib protects the murine liver from ischemia/reperfusion injury. J Hepatol 2012;57:766–73. https://doi.org/10.1016/j.jhep.2012.05.012.

[24] Jun X, Zhen Y, Jinhua Z. Role of NF-kappaB in liver ischemia reperfusion injury of rats. J Huazhong Univ Sci Technol [Med Sci] 2003;23:158–60. https://doi.org/10.1007/BF02859943.

[25] Jiménez-Castro, Cornide-Petronio, Gracia-Sancho, Casillas-Ramírez, Peralta. Mitogen activated protein kinases in steatotic and non-steatotic livers submitted to ischemia-reperfusion. Int J Mol Sci 2019;20:1785. https://doi.org/10.3390/ijms20071785.

[26] Krishnaswamy VR, Korrapati PS. Role of Dermatopontin in re-epithelialization: implications on keratinocyte migration and proliferation. Sci Rep 2015;4:7385. https://doi.org/10.1038/srep07385.

[27] Wei F-F, Trenson S, Verhamme P, Vermeer C, Staessen JA. Vitamin K–dependent matrix gla protein as multifaceted protector of vascular and tissue integrity. Hypertension 2019;73:1160–9. https://doi.org/10.1161/HYPERTENSIONAHA.119.12412.

[28] Rienks M, Barallobre-Barreiro J, Mayr M. The emerging role of the ADAMTS family in vascular diseases. Circ Res 2018;123:1279–81. https://doi.org/10.1161/CIRCRESAHA.118.313737.

[29] Ito S, Yokoyama U, Nakakoji T, Cooley MA, Sasaki T, Hatano S, et al. Fibulin-1 integrates subendothelial extracellular matrices and contributes to anatomical closure of the ductus arteriosus. Arterioscler Thromb Vasc Biol 2020;40:2212–26. https://doi.org/10.1161/ATVBAHA.120.314729.

[30] NERI A-A, DONTAS IA, ILIOPOULOS DC, KARATZAS T. Pathophysiological changes during ischemia-reperfusion injury in rodent hepatic steatosis. Vivo 2020;34:953–64. https://doi.org/10.21873/invivo.11863.

[31] Chang L, Karin M. Mammalian MAP kinase signalling cascades. Nature 2001;410:37–40. https://doi.org/10.1038/35065000.

[32] Hoppstädter J, Ammit AJ. Role of dual-specificity phosphatase 1 in glucocorticoid-driven anti-inflammatory responses. Front Immunol 2019;10. https://doi.org/10.3389/fimmu.2019.01446.
[33] Gao W, Bentley RC, Madden JF, Clavien P-A. Apoptosis of sinusoidal endothelial cells is a critical mechanism of preservation injury in rat liver transplantation. Hepatology 1998;27:1652–60. https://doi.org/10.1002/hep.510270626.
[34] van Golen RF, van Gulik TM, Heger M. The sterile immune response during hepatic ischemia/reperfusion. Cytokine Growth Factor Rev 2012;23:69–84. https://doi.org/10.1016/j.cytogfr.2012.04.006.
[35] Papa S, Bubici C, Zazzeroni F, Pham CG, Kuntzen C, Knabb JR, et al. The NF-κB-mediated control of the JNK cascade in the antagonism of programmed cell death in health and disease. Cell Death Differ 2006;13:712–29. https://doi.org/10.1038/sj.cdd.4401865.
[36] Verzella D, Pescatore A, Capece D, Vecchiotti D, Ursini MV, Franzoso G, et al. Life, death, and autophagy in cancer: NF-κB turns up everywhere. Cell Death Dis 2020;11:210. https://doi.org/10.1038/s41419-020-2399-y.
[37] Kondylis V, Kumari S, Vlantis K, Pasparakis M. The interplay of IKK, NF-κB and RIPK1 signaling in the regulation of cell death, tissue homeostasis and inflammation. Immunol Rev 2017;277:113–27. https://doi.org/10.1111/imr.12550.
[38] Dara L. The receptor interacting protein kinases in the liver. Semin Liver Dis 2018;38:073–86. https://doi.org/10.1055/s-0038-1629924.
[39] Mihaylov P, Mangus R, Ekser B, Cabrales A, Timsina L, Fridell J, et al. Expanding the donor pool with the use of extended criteria donation after circulatory death livers. lt.25462 Liver Transplant 2019. https://doi.org/10.1002/lt.25462.
[40] Schlossberg H, Zhang Y, Dudus L, Engelhardt JF. Expression of c-fos and c-jun during hepatocellular remodeling following ischemia/reperfusion in mouse liver. Hepatology 1996;23:1546–55. https://doi.org/10.1002/hep.510230635.
[41] Shaulian E, Karin M. AP-1 as a regulator of cell life and death. Nat Cell Biol 2002;4:E131–6. https://doi.org/10.1038/ncb0502-e131.
[42] Uehara T, Bennett B, Sakata ST, Satoh Y, Bilter GK, Westwick JK, et al. JNK mediates hepatic ischemia reperfusion injury. J Hepatol 2005;42:850–9. https://doi.org/10.1016/j.jhep.2005.01.030.
[43] Yang X, Lu D, Wang R, Lian Z, Lin Z, Zhuo J, et al. Single-cell profiling reveals distinct immune phenotypes that contribute to ischaemia-reperfusion injury after steatotic liver transplantation. Cell Prolif 2021;54. https://doi.org/10.1111/cpr.13116.
[44] Zhang D, Wang Y, Zeng S, Zhang M, Zhang X, Wang Y, et al. Integrated analysis of prognostic genes associated with ischemia–reperfusion injury in renal transplantation. Front Immunol 2021;12. https://doi.org/10.3389/fimmu.2021.747020.
[45] Hasenfuss SC, Bakiri L, Thomsen MK, Williams EG, Auwerx J, Wagner EF. Regulation of steatohepatitis and PPARγ signaling by distinct AP-1 Dimers. Cell Metab 2014;19:84–95. https://doi.org/10.1016/j.cmet.2013.11.018.
[46] Starmann J, Fälth M, Spindelböck W, Lanz K-L, Lackner C, Zatloukal K, et al. Gene expression profiling unravels cancer-related hepatic molecular signatures in steatohepatitis but not in steatosis. PLoS One 2012;7:e46584. https://doi.org/10.1371/journal.pone.0046584.
[47] Aran D, Camarda R, Odegaard J, Paik H, Oskotsky B, Krings G, et al. Comprehensive analysis of normal adjacent to tumor transcriptomes. Nat Commun 2017;8:1077. https://doi.org/10.1038/s41467-017-01027-z.
[48] Bhogal RH, Mirza DF, Afford SC, Mergental H. Biomarkers of liver injury during transplantation in an era of machine perfusion. Int J Mol Sci 2020;21:1578. https://doi.org/10.3390/ijms21051578.
[49] Wichmann H-E, Kuhn KA, Waldenberger M, Schmelcher D, Schuffenhauer S, Meitinger T, et al. Comprehensive catalog of European biobanks. Nat Biotechnol 2011;29:795–7. https://doi.org/10.1038/nbt.1958.